

Master's Programme in Human Neuroscience and Technology

# Effects of cognitive training in neuronal synchrony - EEG resting state analysis

---

**Emilia Lönnberg**

Master's Thesis  
2021

---

<b>Author</b>	Emilia Lönnberg	
<b>Title of thesis</b>	Effects of cognitive training in neuronal synchrony - EEG resting state analysis	
<b>Programme</b>	Life Science program in the School of Science	
<b>Major</b>	Human Neuroscience and Technology	
<b>Thesis supervisor</b>	Prof. Matias Palva	
<b>Thesis advisor(s)</b>	Prof. Matias Palva	
<b>Collaborative partner</b>	Palva lab, University of Helsinki	
<b>Date</b>	<b>Number of pages</b>	<b>Language</b>
23.12.2021	48	English

---

### Abstract

Computerized cognitive training has been shown to improve cognitive functions such as working memory and cognitive control. This kind of repeated strain on a cognitive system exposes for neuroplastic changes and thereby leads to cognitive improvements. Communication between neural networks is achieved through coherently oscillating neurons. This synchronous communication between neuronal populations is associated with cognitive functions. Detecting and quantifying these rhythmic oscillations of different frequency bands can lead to important insights into the dynamic networks of cognition and behavior. This master's thesis compares the synchronization between pre and post resting states in a cognitive training paradigm. Participants either were randomly divided into the active or control version of the paradigm. Active version consisted of cognitive control, working memory, and mental planning tasks in partially randomized order and control version was a simple psycho-motoric task. Data were collected with continuous electroencephalography (EGI 256 ch HD) and source modeled prior to analysis. Interareal synchronization was summarized as a proportion of significant connections from all possible connections, as a connection density  $K$ . Results showed synchronization differences between the action and control group, where active group had positive connections in the cognitive control and working memory frequency bands. Based on the literature, strengthened theta and alpha activity on the positive connections can be linked to enhanced cognitive control, whereas strengthened theta band activity on the positive connections can be linked to enhanced working memory. However, more research, participants and training data are needed to validate these results. In line with these, results give promising direction for computerized cognitive training, where paradigms can be utilized as a therapeutics for neurological and psychological disorders in the future.

---

**Keywords** Cognitive control, working memory, cognitive training, synchronization

---

---

**Tekijä** Emilia Lönnberg

---

**Työn nimi** Kognitiivisen harjoittelun vaikutukset hermosolujen synkroniaverkostossa – EEG lepomittausanalyysi

---

**Koulutusohjelma** Life Science program in the School of Science

---

**Pääaine** Human Neuroscience and Technology

---

**Vastuopettaja/valvoja** Prof. J. Matias Palva

---

**Työn ohjaaja(t)** Prof. J. Matias Palva

---

**Yhteistyötaho** Matias Palvan tutkimusryhmä (Palva lab), Helsingin yliopisto

---

**Päivämäärä** 22.13.2021

**Sivumäärä** 48

**Kieli** Englanti

---

## Tiivistelmä

Tutkimukset osoittavat, että aivot kykenevät neuroplastisiin muutoksiin tehostaen eri aivoalueiden aktiivisuutta. Kognitiivinen harjoittelu on osoittanut parantavan kognitiivisia toimintoja, kuten työmuistia ja kognitiivista ohjausta. Tämän kaltainen toistuva rasitus kognitiivisessa järjestelmässä johtaa neuroplastisiin muutoksiin ja parantavat kognitiivista ohjausta. Hermoverkoston välinen kommunikaatio saavutetaan yhdenaikaisesti värähtelevien hermosolujen välityksellä. Tämä synkroninen kommunikaatio hermoverkkojen välillä liitetään kognitiivisiin toimintoihin. Näiden eri taajuuksilla olevien rytmisten värähtelyjen havaitseminen ja kvantifiointi on tärkeää kognition ymmärtämiseksi. Tämä diplomityö vertailee kognitiivisen harjoittelun vaikutuksia lepomittausten synkronioissa. Osallistujat jaettiin satunnaisesti joko tutkimusparadigman aktiiviseen tai kontrolliversioon. Aktiivinen versio käsitteli kognitiivisen ohjauksen, työmuistin ja suunnittelun tehtäviä. Kontrolliversio oli puolestaan yksinkertainen psykomotorinen tehtävä. Mittaus suoritettiin elektroenkefalografialla (EGI 256 ch HD) ja lähdemallinnettiin ennen analyysiä. Aivoalueiden välinen synkronointi kuvattiin yhteystiheys K:na, joka kuvaa mahdollisia merkityksellisiä synkronioita aivoalueiden välillä. Tulokset näyttivät synkronointieroja aktiivi- ja kontrolliryhmän välillä, jossa aktiiviryhmä osoitti positiivisia yhteyksiä kognitiivisen ohjauksen ja työmuistin taajuuksilla. Kirjallisuus viittaa, että voimistunut theeta- ja alfa-aktiivisuuden synkronia yhdistetään tehostuneeseen kognitiiviseen ohjaukseen, kun taas theeta-aktiivisuuden synkronia yhdistetään parantuneeseen työmuistiin. Näiden tulosten validoimiseksi tarvitaan kuitenkin enemmän tutkimusta, osallistujia ja mittausdataa. Tulokset antavat kuitenkin lupaavaa suuntaa siitä, mitä jo lyhyellä harjoittelujaksolla voidaan synkroniaverkostoissa saavuttaa. Kognitiivista harjoittelua voidaan täten tulevaisuudessa mahdollisesti hyödyntää entistä enemmän neurologisten ja psykologisen sairauksien terapiamuotona.

---

**Avainsanat** Kognitiivinen kontrolli, työmuisti, kognitiivinen harjoittelu, synkronisaatio

---

## Contents

Preface.....	5
Abbreviations .....	6
1 Introduction .....	7
2 Background.....	11
2.1 Cognitive control .....	11
2.1.1 Task Switching.....	12
2.1.2 Neuronal dynamics in cognitive control .....	12
2.2 Working memory .....	14
2.2.1 Neuronal dynamics in working memory.....	15
2.3 Electroencephalogram .....	16
2.4 Magnetic resonance imaging .....	17
2.5 Independent component analysis.....	19
2.6 Source Modeling.....	21
2.6.1 Head model .....	21
2.6.2 Source Model.....	23
2.7 Imaginary Phase Locking Value.....	23
3 Research material and methods.....	26
3.1 Participants .....	26
3.2 Paradigm .....	27
3.2.1 Active version .....	29
3.2.2 Control version .....	30
3.2.3 EEG Recordings.....	30
3.2.4 MRI Recordings.....	30
3.2.5 EEG Data Preprocessing, Filtering, and Source Analysis.....	31
3.2.6 Analysis and Visualization of Phase Synchrony .....	33
4 Results .....	35
5 Discussion.....	39
6 Summary .....	42
References.....	43

## **Preface**

I want to start by thanking Matias Palva for giving me this amazing opportunity to work in your team and be a part of your research. I also want to thank Joonas Juonen, (aka. Python- and brain-guru), who answered hundreds of my questions day and night.

I want to thank my husband Jan, who supported, loved and helped during this journey of graduation. Last but definitely not least, I want to thank my parents who have supported and rooted during this thesis creation and my whole study at Aalto University.

This work is dedicated for my Babushka.

## Abbreviations

BEM	boundary element model
CC	cognitive control
CO	cingulo-opercular/insular
cPLV	complex PLV
CTC	communication-through-coherence
DA	dorsal attention
EEG	electroencephalography
EF	executive functions
FDR	false discovery rate
FID	free-induction decay
FP	frontoparietal
ICA	independent component analysis
iPLV	imaginary PLV
K	connection density
MRI	magnetic resonance imaging
PFC	prefrontal cortex
PLV	phase locking value
RF	radiofrequency
WM	working memory

# 1 Introduction

Executive functions (EF) refers to top-down neurocognitive processes that are critical in goal-directed behavior (Miyake et al. 2000). EFs are involved in interrelated, but separate processes, such as working memory (WM) and cognitive control (CC) (Miyake et al. 2000; Wang et al. 2019). Higher-order executive functions requires simultaneous use of separate processes and includes planning and fluid intelligence (Miyake et al. 2000). There are several neuropsychological tests (e.g. Stroop Task, Wisconsin Card Sorting Task, N-back Task), which are used as a measure of EFs in research and in diagnosis of neurological and psychiatric disorders.

EFs develop until late adolescence but improves most rapidly during childhood and are linked heavily to structural and functional changes in prefrontal cortex (Zelazo et al. 2012; Nouchi et al. 2013). Computerized cognitive training has gain popularity in the world of entertainment and research, where it is used to improve executive functions (Jaeggi et al. 2017). Task related and task unrelated performance enhancements has been detected before and after cognitive training, especially with individuals of age-related or clinical impairments (Jaeggi et al. 2017).

From various methods of cognitive training, video gaming is one of them (Nouchi et al. 2013). Playing video games leads to transfer effect and improves the performances of other untrained tasks, where previously learned concepts are extended to new concepts (Nouchi et al. 2013). Core-training hypothesis is a potential mechanism for performance enhancements during video gaming, where player's cognitive system is exposed to repeated strain via video game (Waris et al. 2019). Long term repetitions can induce plastic changes in the brain and lead to cognitive improvements (Waris et al. 2019; Bavelier et al. 2012). Commercial brain training games have gain popularity and interest in the development, whereas Nouchi et al. (2013) found that Brain Age (Nintendo Co. Ltd) improved cognitive functions.

Video games differ perceptually, attentionally and visually from 'classical' training paradigms (Green et al. 2008): In video games, players are moving and interacting as an avatar in a three dimensional ecologically valid manner (Achtman et al. 2008), whereas in classical training paradigms, squares are identified based on orientation, amount and color (Green et al. 2008). Studies have shown how participants use similar underlying processes in video gaming and in classical training paradigms (Green et al. 2008). However, video games differ many ways from classical training paradigms. Classical training paradigms do not demonstrate transfer effects as video games do (Green et al. 2008). Training paradigms lack the complexity of motor responses, where pressing two buttons is not as detailed coordination as in video games (Achtman et al. 2008). These motor responses are important for plastic changes, where studies have witnessed the large scale changes in motor functions induced by training (Achtman et al. 2008). Classical learning paradigms are based on repeated specific solutions where only minor orientations are changed (Green et al. 2010). The effects of playing video games on cognitive skills are recognized, where enhancements in perception, attention and in cognitive control are resulted (Green et al. 2015)

Communication-through-coherence (CTC) is crucial part of synchronous communication (Jensen et al. 2014). This hypothesis proposes that sender and receiver neural networks communicate via coherently oscillating neurons (Helfrich et al. 2016). Synchronous fronto-parieto-occipital and fronto-temporal communication has been linked to cognition and behavior (Helfrich et al. 2016). Thus, delta (1–4 Hz), theta (4–8 Hz), and alpha (8–14 Hz) frequency bands are connected to large-scale cognitive processes (Palva et al. 2011)



In the present work, I investigated whether newly constructed cognitive training paradigm would show differences in neuronal synchronization between pre and post resting states. Study paradigm has inspired its ecological manner from video games and has first-person shooter, puzzle game and problem solving elements. Paradigm was designed to train cognitive control, working memory and mental planning, all performed in varying task forms.

This master's thesis studies the effects of cognitive training paradigm on the neuronal synchronization between pre and post resting states. To study the effectiveness of the paradigm, participants were randomly divided into active or control version of the paradigm. Active version consisted cognitive control, working memory, and mental planning tasks in partially randomized order and placebo version was simple psycho-motoric task. Data were collected from 8 participants with continuous EEG (EGI 256 channel HD) and source modeled prior to analysis. Interareal synchronization was summarized as a proportion of significant connections from all possible connections, as a connection density  $K$  (Palva and Palva. 2012; Hirvonen et al. 2017).

The main hypotheses of this study are:

- Shown differences in phase synchronization between the action and control group
- Enhanced activity of cognitive control and working memory frequency bands

This study has been divided into 3 following chapters. Background will cover the basics of cognitive control and working memory, electroencephalography and magnetic resonance imaging. Also, methods used for the preprocessing of electroencephalography data, like independent component analysis, source modeling and phase locking values, are described more detailed way. Methods-section covers more precise description of the study paradigm, measurement and data processing. Discussion of the presented results are described with attention to detail, whereas all are summarized in the final chapter.

## **2 Background**

Adult's brain is capable for neuroplastic changes when challenges are faced (Morimoto et al. 2014). Computerized cognitive training has been shown to improve cognitive control, working memory and task shifting (Morimoto et al. 2014). Studies have witnessed the increasing use of digital therapeutics, inspired by game-like components to treat cognitive deficits (Välimäki et al. 2021). These so called therapeutic games have elements activating challenge, motivation and reward systems and potentially can be used for cognitive deficits treatment (Li et al. 2014).

### **2.1 Cognitive control**

The ability to maintain attention during work, the ability to not to scratch a mosquito bite, or the ability to play chess require cognitive control (CC). CC guides thought and behavior based on goals and motivation, through competing responses (Rougier et al. 2005; Parro et al. 2018). CC is involved with several related processes, which include working memory, error detection, inhibition, abstract thought and reasoning, and rule shifting (Koster et al. 2008; Parro et al. 2018). CC is flexible and allows us to process information and behavior over time depending on goals and perform novel tasks with almost nonexistent experience (Koster et al. 2008; Rougier et al. 2005).

CC depends highly on the function and development of prefrontal cortex (PFC) (Chevalier et al. 2019), where the representations of rules and goals are provided by top-down influences over motor and perceptual systems to guide actions (Rubia et al. 2006; Riddle et al. 2020). CC have been shown to develop throughout adolescence and reach its full potential in the individuals 20's (Rubia et al. 2006; Rougier et al. 2005).

### **2.1.1 Task Switching**

Adaptive behavior allows humans to select, maintain and categorize relevant information and suppress irrelevant ones. On the other hand, it allows us to recategorize information, if previously irrelevant information becomes relevant. This being said, humans are adapting attention, thought and action toward goals and motivation. When new goals emerge, previous factors for old goals are replaced, a process referred to task switching (Riddle et al. 2020).

Rostral prefrontal cortex is involved in the control of rules, goals, and contexts (Riddle et al. 2020). Cognitive control determines the most suitable rule towards current goal among from competing alternative rules (Riddle et al. 2020; Cooper et al. 2020). Task switching is crucial in video game training and can be used as an operationalization for cognitive control (Karle et al. 2009).

### **2.1.2 Neuronal dynamics in cognitive control**

Cognitive control is formed from large-scale functional networks, which activate when cognitive challenges are faced (Sadaghiani et al. 2017). Cognitive control networks can be localized, which include cingulo-opercular/insular (CO) network, frontoparietal (FP) network, and a dorsal attention (DA) network, all identified in the Figure 1.

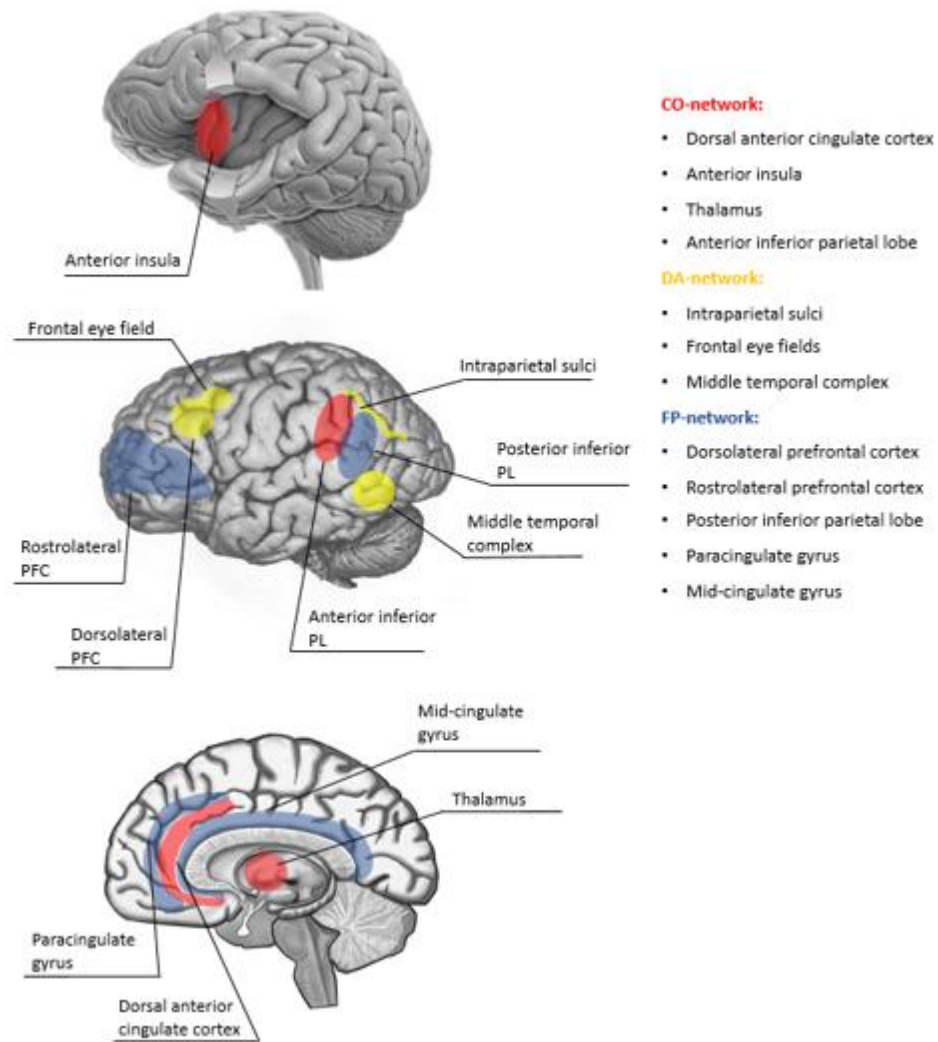


Figure 1. The CO- (red), DA- (yellow) and FP-network (blue) are crucial functional locations in cognitive control (Sadaghiani et al. 2017). (Images modified from Vaskovic. 2021 (Insular lobe), Jeudi. 2021 (Cortex), Sousa et al. 2011 (Medial))

Neuronal oscillations have functional significance for the large-scale neuronal interactions underlying cognition (Varela et al. 2001). Cognitive functions are associated with rhythmic oscillations of different frequency bands, generated by distinct biophysical mechanisms (Riddle et al. 2020). Theta band (4 – 8 Hz) oscillations are observed in hippocampus during memory formation (Huycke et al. 2020) and in the cerebral cortex of the frontal-medial cortex (Sauseng et al. 2019). Also, alpha band

(8-12 Hz) activity is observed in cognitive control (Huycke et al. 2020; Palva et al. 2011). Amplitude and phase of alpha band oscillations regulate signal processing by shaping perception and cognition (Sadaghini et al. 2017). Alpha band allows us to process current information effectively by blocking irrelevant processing pathways in task-irrelevant brain areas (Mazaheri et al. 2009).

## **2.2 Working memory**

Working memory (WM) is a short-term memory system that is used for the execution of cognitive tasks (Cowan et al. 2014). WM is connected to higher cognitive functions like intelligence, conscious thought processes, decision making, information processing, comprehension, problem-solving and learning (Cowan et al. 2014; Alagapan et al. 2019; Waris et al. 2019). WM is a crucial part of daily functioning, holding and manipulating information, which affects humans and animals in all age groups. Poor WM is associated with poor functional outcome (Välimäki et al. 2021).

Working memory has a limited capacity of three to four objects and is capable holding information only temporally (Palva et al. 2011). Yet, WM involves cognitive processing in parallel that access 'infinite' long-term memory system (Sauseng et al. 2020). WM is thought to be divided into two storage systems, where one is for the verbal and one is for the visual material (Sauseng et al. 2020). Human's visual working memory (VWM) capacity is limited and retains only small amount of information (Sauseng et al. 2020), but is critical during learning, solving novel tasks or acquiring new knowledge (Blacker et al. 2014). However, the visual environment is extremely overloaded, where information is either retained or suppressed by the viewer (Blacker et al. 2014; Sauseng et al. 2020). Visual information is retained or suppressed by the neural oscillations of the prefrontal and posterior parietal cortex (Riddle et al. 2020).

### 2.2.1 Neuronal dynamics in working memory

Frontoparietal connectivity is believed to be functional component of WM, whereas frontal and temporal regions are connected with WM task performance (Alagapan et al 2019). In addition, task-related WM activity has been shown in the PFC, parietal cortex, striatum, cerebellum, basal ganglia and medial temporal lobe (Eriksson et al. 2015), all identified in the Figure 2.

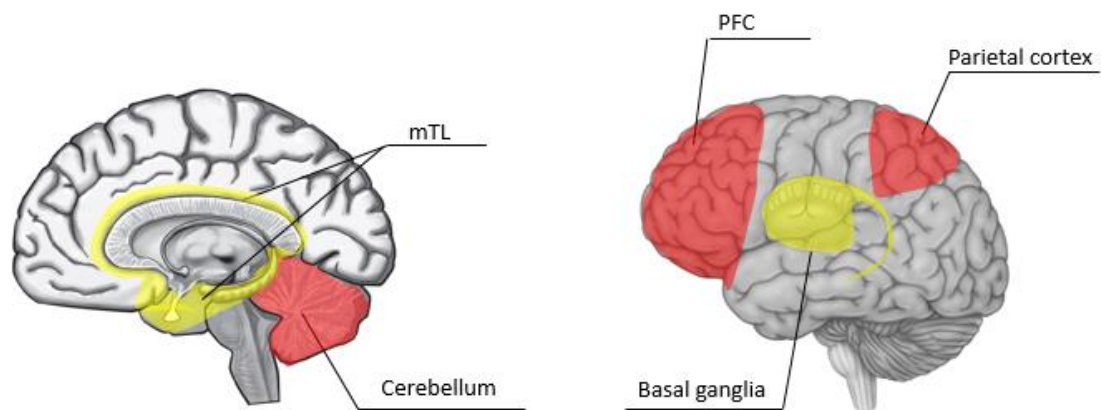


Figure 2. Task related WM connectivity areas can be identified as: PFC, parietal cortex, striatum, cerebellum, basal ganglia and medial temporal lobe (Eriksson et al 2015). (Image modified from Jeudi. 2021 (Cortex); Sousa et al. 2011 (Medial))

During the recent decade, studies have focused on human electroencephalographic (EEG) theta (4 –8 20Hz) and alpha (8 –12 Hz) activity and its importance in spatial navigation, memory processes and attention (Sauseng et al. 2010). Different oscillating frequency bands can identify frontoparietal connectivity, where the load of WM task activates the synchronization of the alpha band (Alagapan et al. 2019). In addition, memory-related theta activity is one of the most reported frequency bands concerning long-term and working memory (Sauseng et al. 2010).

## 2.3 Electroencephalogram

The electroencephalogram (EEG) is old, inexpensive and portable technique to measure neuronal activity. EEG can be used for clinical diagnosis for the identification of epilepsy and sleep disorders (Michel et al. 2019). Scalp's electrodes of EEG measure secondary volume currents of pyramidal cells (Beres. 2017) (Figure 3).

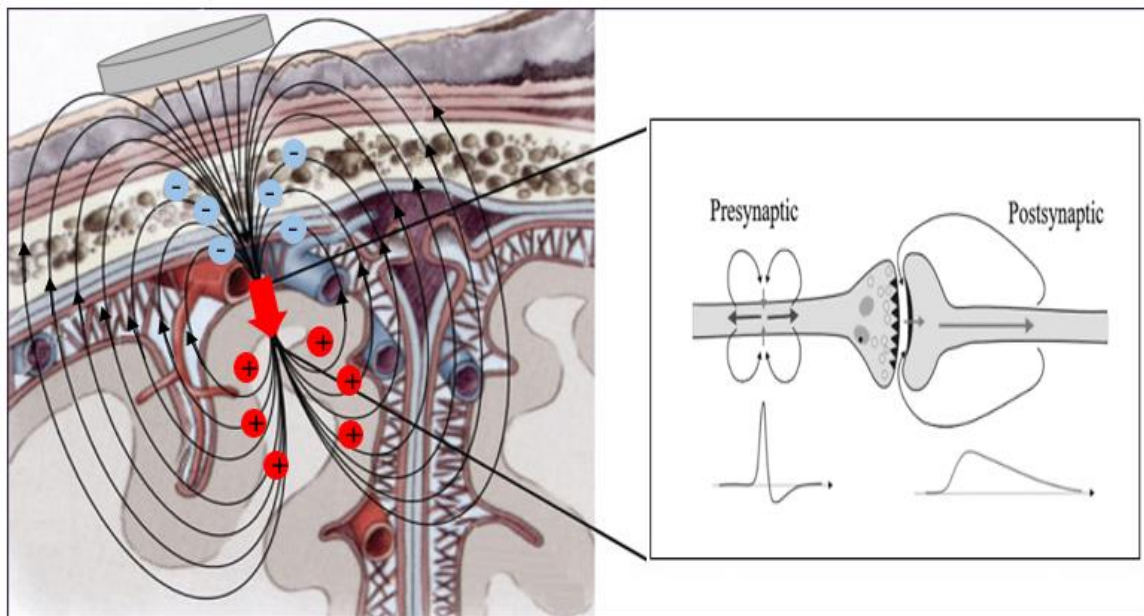


Figure 3. Electrode is placed on the scalp and red arrow represents generator. EEG measures secondary volume currents of pyramidal cells, where postsynaptic potentials are the main source of signals (Sandor et al. 2020). (Image modified from Sandor et al. 2020; Beres et al 2017).

Figure 3 shows two types of synapses: presynaptic action potentials and postsynaptic potentials, where postsynaptic potentials are the main source of EEG signals. Postsynaptic potentials activate in the postsynaptic membrane by the ligand-gated ion channels, or ionotropic receptors, whereas the action potentials activate in the axon hillock by the voltage-gated ion channels (Beres et al. 2017). Postsynaptic potentials change the electrical charge from the outside of the membrane (Beres et



al. 2017). Change of the membrane charge lasts about 200 milliseconds, which is long enough for EEG electrodes to detect (Michel et al. 2019). Due to the briefness and speed of the action potentials, EEG electrodes are too slow to detect them (Michel et al. 2019).

EEG reveals oscillations rising from and within the brain in different frequency bands, such as delta (1-3 Hz) theta (4–8 Hz), alpha (8–12 Hz), beta (13-30 Hz), gamma (30–100 Hz) and high-frequency oscillations (100–200 Hz) (Fitzgerald et al. 2018). However, EEG has difficulties to locate the brain areas that generate specific neuronal activity (poor spatial resolution) (Michel et al 2019). Thus, it is preferable that EEG data are combined with detailed and truthful model of the head anatomy and source modeled prior to analysis (Michel et al. 2019).

## **2.4 Magnetic resonance imaging**

Spin induces magnetic field around Hydrogen and Phosphorus nucleus (Westbrook et al. 2011). Spin depends on the number of protons and does not induce magnetic energy directly to nucleus, but affects to its surrounding parts (Grover et al. 2015). When an external magnetic field ( $B_0$ ) is introduced, nuclear spins align with the external field in parallel or in perpendicular to the external field (Figure 4) (Grover et al. 2015).

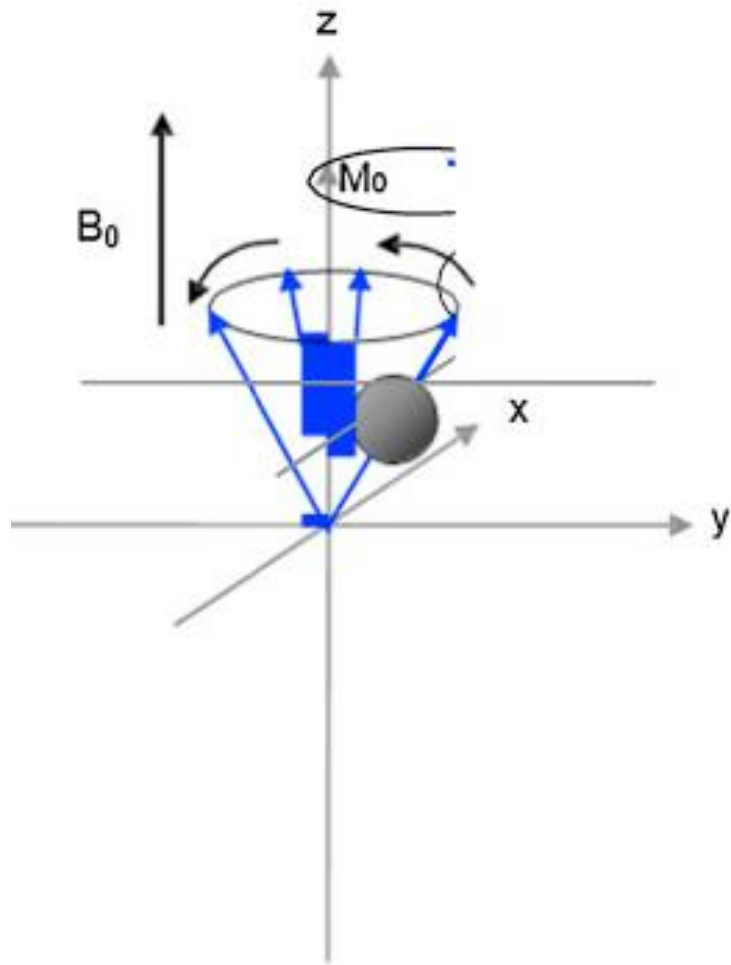


Figure 4. Nucleus spins around the external magnetic field ( $B_0$ ).  $M_0$  is the direction of net magnetization (Grover et al. 2015).

When external magnetic field  $B_0$  is introduced, the nuclei can be excited with additional magnetic field  $B_1$ , which is generated by the radiofrequency (RF) (Grover et al. 2015). The energy absorbed from RF induces a voltage, that generates free-induction decay (FID) (Grover et al. 2015). In practice, RF pulses are applied to generate multiple FIDs, which are averaged and calculated by Fourier transformation, which finally leads to an magnetic resonance image (Grover et al. 2015).

## 2.5 Independent component analysis

Imagine a room with several microphones in it. One microphone does not only catch one sound source but it is a mix of different sounds at varying levels. One wants to separate the sounds sources and uses Independent Component Analysis (ICA) based on their statistical impendence. Measuring brain signals with EEG faces the same problem: electrodes in the scalp do not only catch measured brain signals, but also mix of unwanted artifacts, like blinks, particular eye movements, heart-beats, and muscle movements (for ex. swallowing). ICA is used for detecting, excluding and correcting statistically independent and non-gaussian artifact signals and reconstructing new ones (Michel et al. 2019). ICA estimates a version of the original signal by multiplying the data by a mixing matrix (Figure 5) (Dariusz et al. 2020). A vector of source signals  $s$  is calculated from the Equation 1:

$$x = As \tag{1}$$

where  $x = (x_1, x_2)$  is a vector of observed signals,  $A$  is an mixing matrix of the number of channels and the number of the source signals, and  $s = (s_1, s_2)$  is a vector of source signals (Dariusz et al. 2020). The number of source signals,  $x$ , is equal to the number of observed signals,  $s$  (Dariusz et al. 2020)

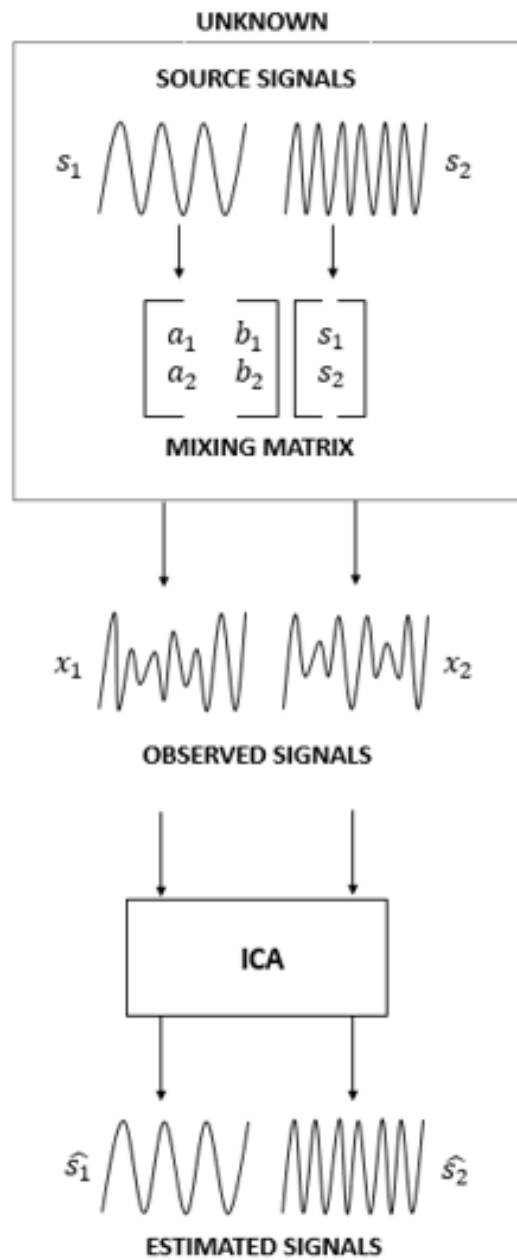


Figure 5. Diagram from the analysis steps of independent component analysis. (Image modified from Dariusz et al. 2020)

## **2.6 Source Modeling**

Source modeling attempts to localize the particular type of activity in the brain (Congedo et al. 2011). To do that, it requires defining a source model and a head model. The head model is used for calculating the forward solution, whereas the forward solution provides the lead field matrix, which is used to solve the inverse problem.

### **2.6.1 Head model**

Constructing a head model needs understanding on how electric currents flow from sources to scalp surface. Current flow depends on the head's geometry and tissue's conductivity (Michel et al. 2019). Skull's resistivity attenuates current flow (Liu et al. 2006). Attenuation and source of the signal determines the scalp's electrode potential (Michel et al. 2019). Coregistration of exact position of each EEG electrode is crucial when building the head model. The head model is based on structural magnetic resonance imaging (MRI), where MRI image reveals the information about the shape of the head, the thickness of the heterogeneous skull and the volume of the gray matter (Michel et al. 2019). MRI image has different coordinate system, hence careful tuning of EEG electrodes to MRI image is important, because coregistration is the foundation of the correct lead field (Michel et al. 2019).

One of the most used model for forward problem is the Boundary Element Model (BEM) (Barnard et al. 1967). BEM calculates the potential by a given source (dipole) at the interfaces and boundary of the volume (Hallez et al. 2007). The interfaces separates regions based on volume conductivity, whereas the boundary separates the non-conducting air with the conducting volume (Hallez et al. 2007). The separation of the volume conduction and source effect can be described as following (Oostenveld et al. 2002):

$$\varphi = A\varphi_{\infty} \quad (2)$$

where  $\varphi$  is the surface potential,  $A$  is a matrix dependent on the volume conductor's geometric and conductive properties and  $\varphi_{\infty}$  is the source term of the infinite medium potential (Oostenveld et al. 2020). A matrix is calculated only once, which makes using BEM computationally fast and popular for its low computational needs (Oostenveld et al. 2020). Derivation of the formula 2 can be found from Mejis et al. 1989. Usually BEM model consist of 3 surfaces: head, inner skull and outer skull, as seen in figure 6. The regions between the interfaces are homogeneous isotropic conducting regions, where interfaces are covered with small boundary elements (Hallez et al. 2007).

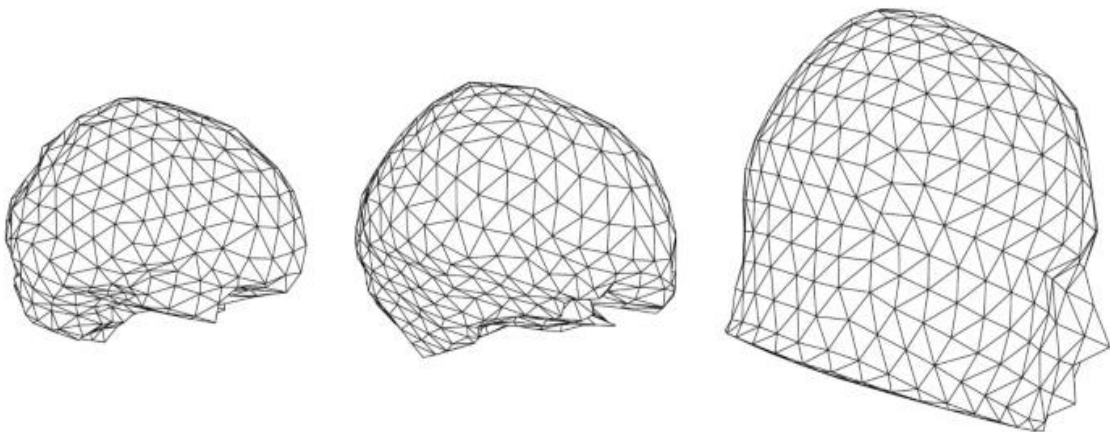


Figure 6. Three surfaces of BEM-model, which consist of inner skull (left), outer skull (middle) and head (right) surfaces (Hallez et al. 2007).

## 2.6.2 Source Model

As mentioned above, fidelity of the inverse solution depends crucially on the forward model and constructed lead field (Liu et al. 2006). Lead field determines electrode's electric activity and studies source activation to potentials at sensor location (Liu et al. 2006). A source model is defined by the 3D positions of dipoles on the cortical surface (Michel et al. 2019). Signals are generated by dipoles, also referred as source space.

Inverse problem is solved by localizing the dipoles, where the number of dipoles depends on the number of scalp electrodes. Solution makes an assumption that the source of the potential field in the scalp is generated only few active areas in the brain (Michel et al. 2019). Dipole estimation is crucial for the source model: underestimation of the dipoles makes the source localization biased, whereas overestimation of the dipoles exposes the source localization to spurious sources (Michel et al. 2019).

## 2.7 Imaginary Phase Locking Value

Phase relationships are used as a measurement of functional connectivity (Lachaux et al. 1999), where two phased brain areas have related oscillation properties (Bruña et al. 2018). Phase locking value (PLV) is one of the most used mathematical operationalization of phase connectivity analysis (Lachaux et al. 1999). PLV evaluates the constant phase difference between two connected areas, where signals are so called locked to each other (Lachaux et al. 1999). In order to find PLV values that are statistically significant, surrogated trials are shuffled in one of the channels (Figure 7):

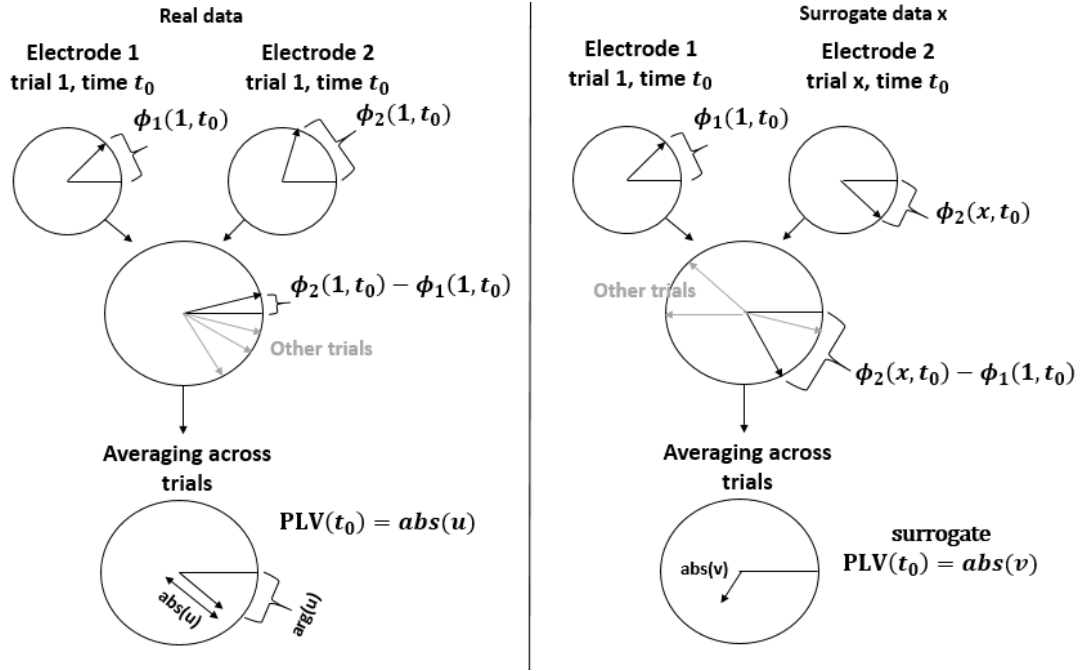


Figure 7. Estimation of PLV. Left: Synchrony is related to the phase difference between electrode 1 and 2. Amplitude  $abs(u)$  (PLV) with latency  $t$  is calculated by averaging phase differences across trials. Right: Surrogate data are constructed by shuffling the trials of one of the electrodes. Amplitude  $abs(v)$  (PLV) with latency  $t$  is calculated by averaging phase differences across trials. (Lachaux et al. 1999). (Image modified from Lachaux et al. 1999)

PLV gives understanding on the relationship between frequencies and network communication (Schmidt et al. 2014). In addition, PLV allows deviation to its 'constant' phase difference because brain signals come across noisy and it is not always accurate whether the signal comes only from one oscillator (Bruña et al. 2018). The PLV is the absolute value of complex PLV,  $cPLV$  ( $PLV = |cPLV|$ ), where  $cPLV$  can be defined as following:

$$cPLV = \sum_{t=1}^N [e^{i(\theta_X(t) - \theta_Y(t))} / N] \quad (3)$$



where  $N$  is the sample number,  $\theta_x/\theta_y$  are phases of time series of  $X$  and  $Y$  (Lachaux et al. 1999; Palva et al. 2005). Values range between 0 and 1, indicating that values closer to 1 has better phase synchronization. However, several sensors can measure the same sources and are sensitive to source effects, like volume conduction and source leakage due to EEG's low spatial resolution (Palva et al. 2005; Yoshinaga et al. 2020). These source effects cannot be entirely solved with ICA (Yoshinaga et al. 2020) and are problematic, when they occur with zero-lag propagation, meaning the spurious phase difference is zero among signals (Palva et al. 2005; Yoshinaga et al. 2020).

Imaginary PLV (iPLV) reduces the source effects by discarding zero-lag connectivity (Yoshinaga et al. 2020). iPLV is not sensitive to linear mixing caused by volume conduction (Arnulfo et al. 2020). iPLV is an absolute imaginary part of  $cPLV$  ( $iPLV = |Im(cPLV)|$ ) and can be defined as following:

$$iPLV = | \text{Im} \sum_t e^{i(\theta_x(t) - \theta_y(t))} / N | \quad (4)$$

iPLV does not take account artificial synchrony, but at a cost can ignore true zero-phase lag interactions (Palva et Palva. 2018).

### 3 Research material and methods

#### 3.1 Participants

7 participants (4 female, 3 male) with ages ranging from 26-38 years (mean age =  $31.25 \pm 2.35$ ) participated in this study. Subjects were recruited from the University of Helsinki. All participants had normal vision, were right-handed and had no diagnosed psychiatric or neurologic disorders (Figure 8). In addition, participants were asked about their previous gaming experience and especially about previous first-person shooter game type experience (Figure 9).

Participant	Gender	Age	Handedness	Group
1	M	28	R	Active
2	M	38	R	Active
3	F	28	R	Control
4	F	26	R	Active
5	F	29	R	Control
6	M	28	R	Control
7	F	26	R	Control

Figure 8. Participant statistics consisted of gender, age, handedness and randomized paradigm group.

<b>Participant</b>	<b>Previous Gaming Experience</b>
1	Intense gaming experience, especially from FPS-games
2	Some experience from FPS-gaming
3	Non-existing FPS-gaming experience
4	Some experience from FPS-gaming
5	Non-existing FPS-gaming experience
6	Intense gaming experience, especially from FPS-games
7	Some experience from FPS-gaming

Figure 9. Previous gaming experience was defined, where participants were classified either with non-existing experience, some experience or intense experience.

Participants were randomly assigned to either an active WM, CC and planning task condition (active group) (mean age = 30,67±3.71, 1 man, 2 women) or to a placebo condition (control group) (mean age = 28, 2 men, 2 women).

### **3.2 Paradigm**

The experimental arena was a constrained, flat and perceptually three-dimensional space, where the participant moved and interacted in an ecologically valid manner. There were two, adaptive experimental paradigms, active and control version. Active version consisted tasks for CC, WM and planning with first-person shooter (FPS), real time strategy and puzzle game elements. Control version was a FPS featured paradigm without executive function tasks (Figure 10).

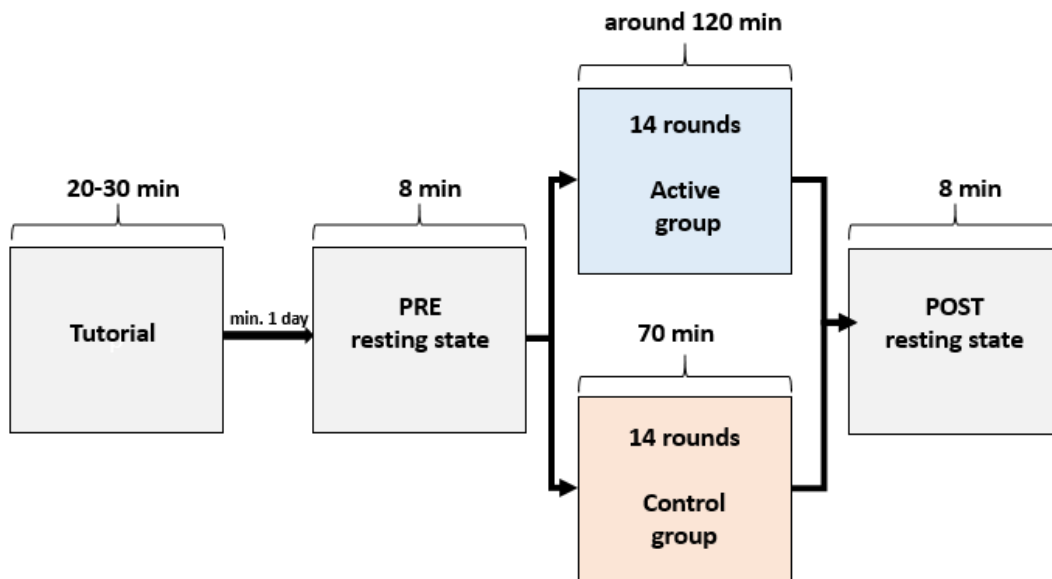


Figure 10. Measurement pipeline.

Paradigm consisted of rounds, whose laptime differed depending on the experimental group. After each round, paradigm was adapted suitable for the participant's level. Active version's round consisted of 10 sub-rounds, which took an average of 6-8 minutes to complete, depending on the player's skill and adaptation level. Control version's laptime was a constant 5 minutes.

Participants performed pre-measurement tutorial minimum 1 day before the actual measurement. In tutorial, participants were verbally instructed for control-use and paradigm rules. In addition, pre-measurement tutorial adapted participants starting level suitable for the participant's skills. Participants practiced tutorial minimum 2 adaptive rounds, lasting about 20-30 minutes.

### 3.2.1 Active version

The active version of paradigm consisted of three blocks: CC task, and two randomized sub tasks activating either WM, VWM or planning (Figure 11)

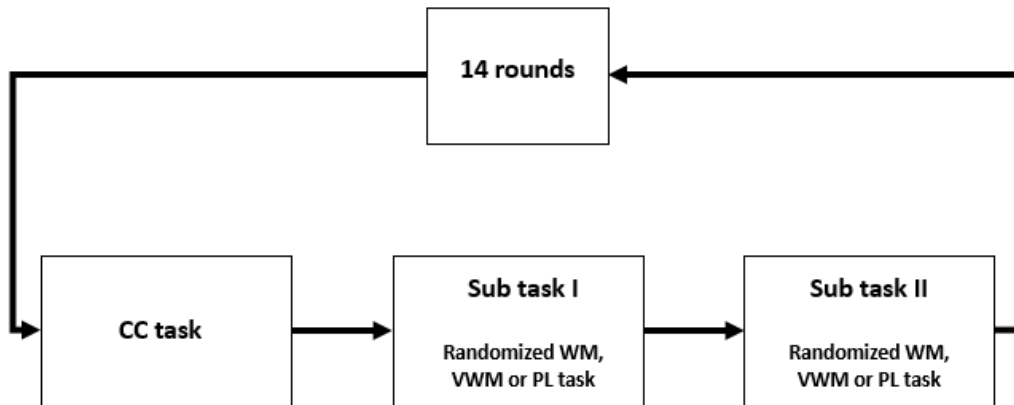


Figure 11. Blocks of the active version.

Three blocks of the paradigm were repeated 140 times. First block was a cognitive control task where the participant interacted with an enemy in a similar manner as in the FPS games. Participant had three possible interaction states with a distinct rule for each state. Participants were instructed about the rules and change of interaction state was visually cued. Deviation from the rules led to cognitive control errors, which were monitored during the experiment. Also, succeeding at the rule changes led to success signals, which were monitored during the experiment. Success and error signals were used to adapt the individual performance.

After the first block, paradigm continued to two randomized sub tasks. Sub tasks were randomly assigned between three different task types: working memory task, spatial configuration visual working memory task and planning task. Randomization was calculated in a manner that each type of sub task appeared equal amount. Sub tasks had puzzle game and problem solving elements.

### **3.2.2 Control version**

In control version, participants interacted with enemies in a similar manner as in the FPS games. Lap time remained constant in 5 minutes. Unlike in active version, control version did not consist of cognitive control, working memory, spatial configuration visual working, or planning tasks. After every round, paradigm was adapted to player's skill level.

### **3.2.3 EEG Recordings**

EEG was recorded using a 256-channel Geodesic Sensor Net (Electrical Geodesics, Inc., Eugene, OR) and EGI software (Electrical Geodesic, Inc., Eugene, OR). Each subject was asked to sit in an armchair in a quiet room. The experiment began with a 8-min eyes open resting state. Each subject was given instructions to visually fixate on a small cross, in order to reduce blinking and lateral eye movement artifacts. Depending on the experiment type (active or control), measurement continued to paradigm and followed up with a 8-min eyes open post resting state. EEG sampling frequency was 1000 Hz. Impedances were kept below 50 k $\Omega$ . The recorded data were high- and low-pass filtered on-line, using 1.0 Hz high-pass and 100 Hz low-pass filtering. EEG electrode locations were digitized using a stereo-camera tracking device (GeoScan Sensor Digitization Device, Philips Neuro Inc., Eugene, OR).

### **3.2.4 MRI Recordings**

For cortical surface reconstructions, individual T1-weighted anatomical MRI scans were obtained at a resolution of 1  $\times$  1  $\times$  1 mm with a 3-T MRI scanner (Siemens, AMI-Center, Espoo).

### 3.2.5 EEG Data Preprocessing, Filtering, and Source Analysis

Preprocessing was started by excluding visually bad channels. Flat and noisy channels were manually deleted. Also, segments were cropped to timescale from 20 seconds of the start of the measurement to 450 seconds. In order to identify and remove artifactual activity from the data, independent component analysis (Picard), with 100 components, was used for all subjects. Exclusion was based on channel detection, spatial pattern, segment image, spectrum plot and segment distribution (Figures 12 and 13).

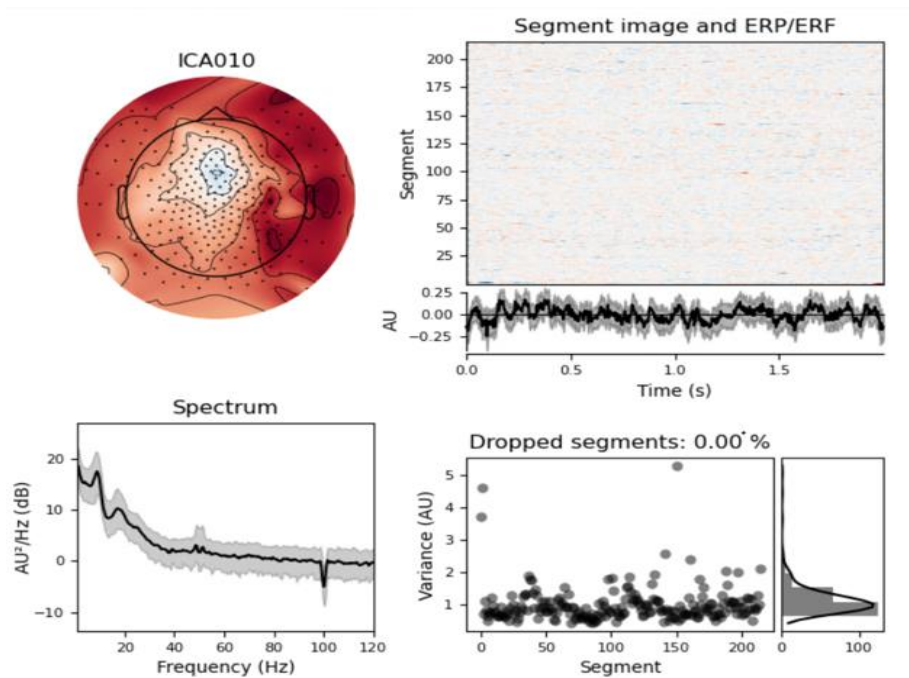


Figure 12. Good example of ICA component. Spatial pattern shows activation on the prefrontal cortex and spectrum peak shows peak at the lower frequency band.

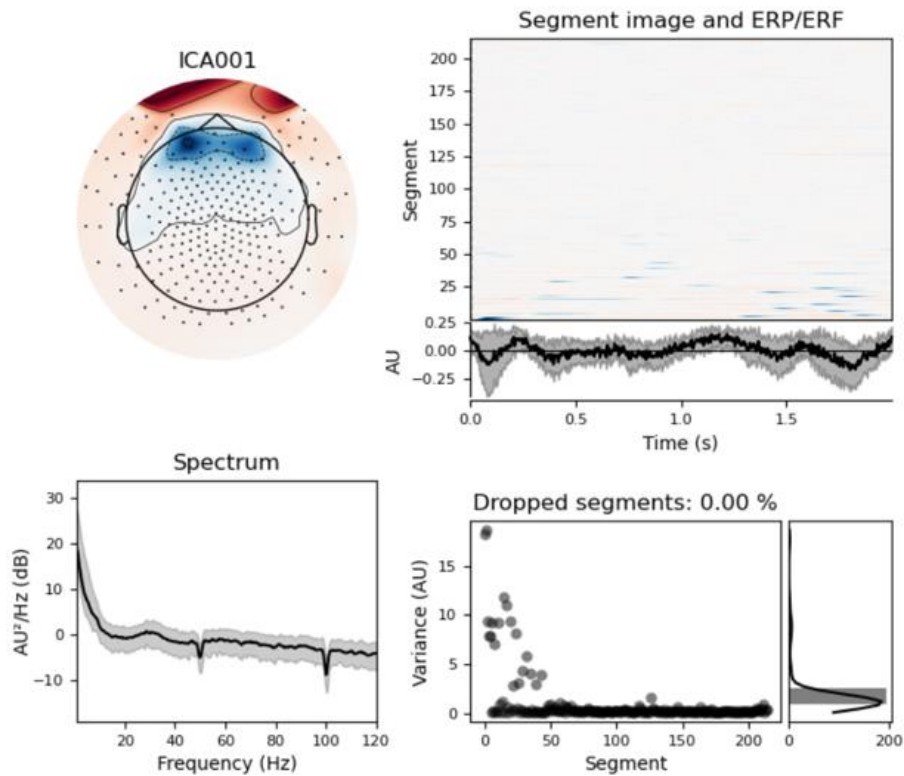


Figure 13. Excluded ICA-component. Spatial pattern shows activation near eye-area.

FreeSurfer software (<http://surfer.nmr.mgh.harvard.edu/>) was used for volumetric segmentation, surface reconstruction, flattening, and labeling. In addition, FreeSurfer software and individual T1-weighted MRI scans was used for cortical parcellations. Parcellations was done by Schaefer parcellations at 200-parcel resolution, where each parcel was assigned to one of seven Yeo functional systems.

The MNE toolkit (<http://www.nmr.mgh.harvard.edu/martinos/userInfo/data/sof-MNE.php>) was used to create three-layer BEM, source models, coregistration (Figure 14) and to calculate forward model and MNE inverse operators (Hämäläinen & Ilmoniemi, 1994).



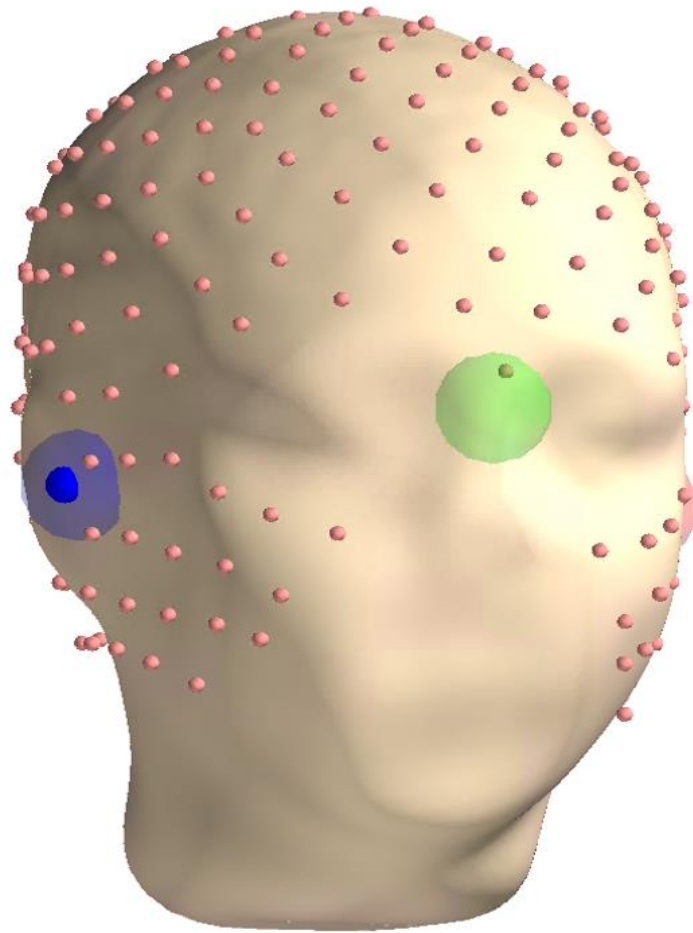


Figure 14. Coregistration of the head model. Residuals were fitted more properly.

### 3.2.6 Analysis and Visualization of Phase Synchrony

The cPLV was estimated between all parcels. Also,  $iPLV = |\text{im}(cPLV)|$ , was evaluated (Eq. 4). iPLV is not sensitive near zero-phase lags like PLV (Brooker et al. 2014), and yields only phase-lagged interactions and their false positive spurious interactions (Wang et al. 2018).

To estimate the statistical significance of synchronization, nonparametric permutation statistics was used. The difference in mean iPLV between pre and post resting state within each pair of parcels was computed. Pre and post resting state were analyzed as trials, where they were randomly redistributed and computed as the mean PLV between permuted conditions. Permutations were repeated 1000 times. The shuffled trial data eliminated nonstimulus-locked synchronization and signal-mixing caused artificial couplings (Lachaux et al. 1999).

Connection density  $K$  was used as a visualization tool for synchrony analysis. Connection density  $K$  summarizes the proportion of significant connections from all possible connections (Palva and Palva. 2012; Hirvonen et al. 2017).

## 4 Results

Interareal synchronization was summarized as a proportion of significant connections from all possible connections, as a connection density  $K$  (Palva and Palva, 2012; Hirvonen et al. 2017). Figures 15 and 16 represent the post and pre resting state iPLV values, averaged over subjects. Colors represents the connection densities of positive ( $K+$ ) and negative ( $K-$ ) observations. Red represents statistically significant fractions of positive connections and blue represents statistically significant fractions of negative connections.

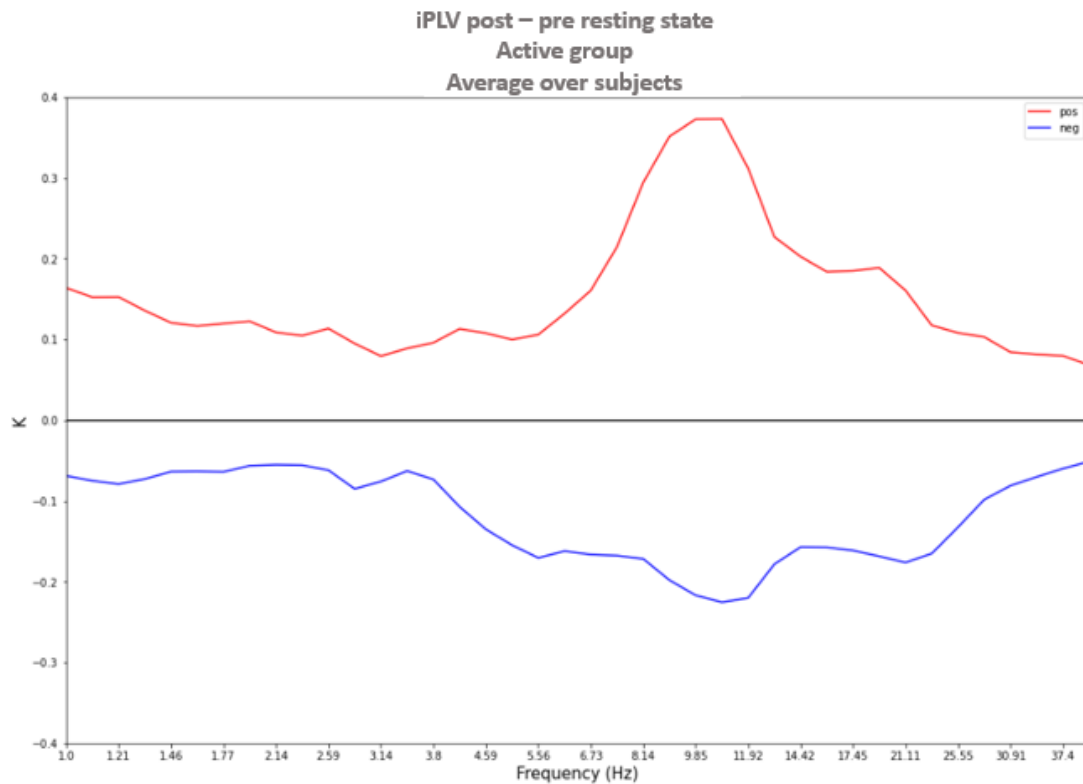


Figure 15. Connection density  $K$  as a function of frequency Hz. Averaged iPLV values over subjects. Post and pre resting state measurement from the active group.

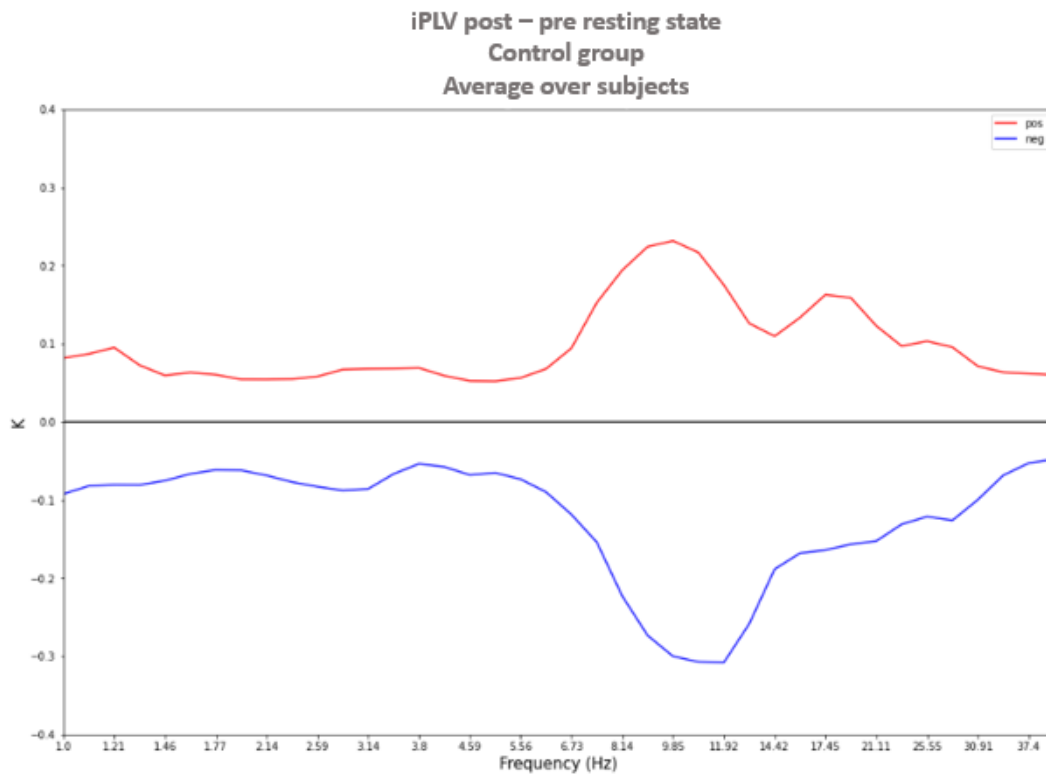


Figure 16. Connection density K as a function of frequency Hz. Averaged iPLV values over subjects. Post and pre resting state measurement from the control group.

Two groups, active and control, had differences in phase-synchronization in several frequency bands. Synchronization was compared between delta ( $\delta$ , 1 - 3 Hz), theta ( $\theta$ , 4 – 8 Hz) and alpha ( $\alpha$ , 8 – 12 Hz) frequency bands and the lower beta ( $\beta$ , 13 – 20 Hz) and lower gamma ( $\gamma$ , 30 – 40 Hz) frequency bands.

Connection densities of the positive observations showed small enhancement in synchronization in the delta and theta frequency bands within the active group. The most noticeable difference between synchronization differences was shown in alpha frequency band, which correlated stronger synchronization in the active group. Lower beta and gamma bands did not show remarkable differences between two groups. Connection densities of the negative observations show stronger theta frequency in the active group and stronger alpha frequency in the control group.

Addition to this, differences in a single-subject level was analyzed. Figures 17 and 18 represent the post and pre resting state iPLV values, represented on a single-subject level. Fractions of connections with a statistically significant positive difference and fractions of connections with a statistically significant negative difference were presented. One color represents the same subject on the positive and negative connections.

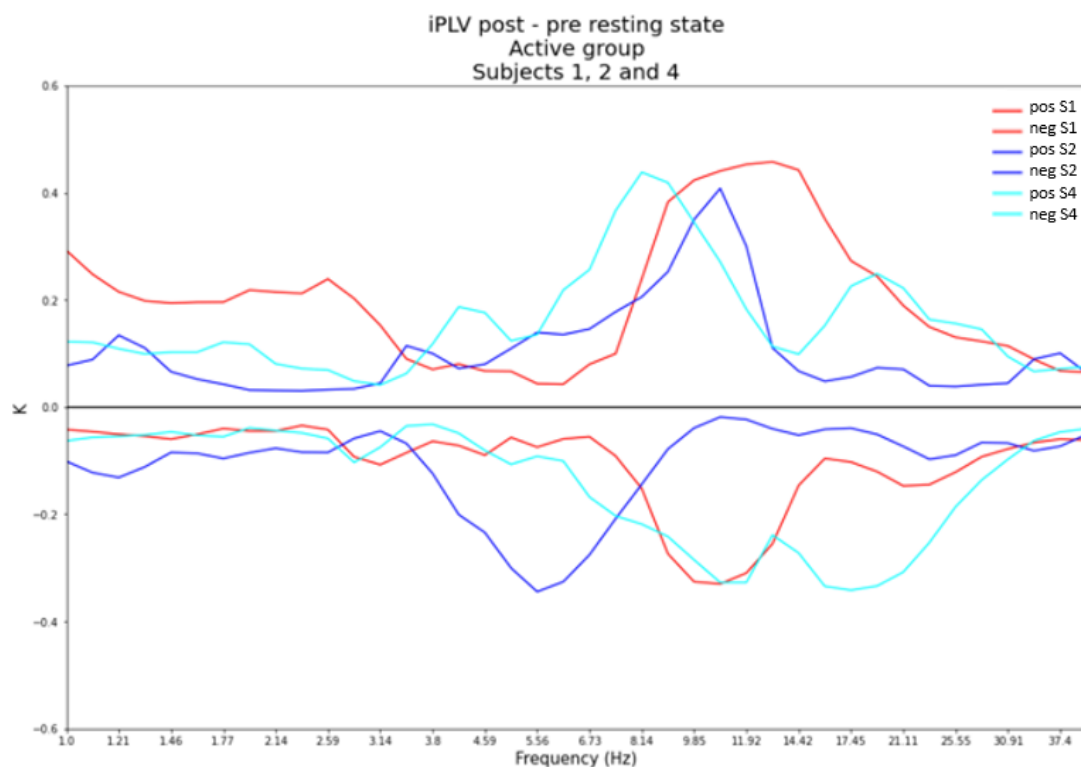


Figure 17. Connection density K as a function of frequency Hz. Single-subject iPLV values. Post and pre resting state measurement from the active group.

All participants in the active group showed larger positive connections in the alpha band and some enhancements in the theta band within subject 2 and 4. In negative connections, subjects 1 and 4 showed larger negative connections in the alpha band and subject 2 showed larger negative connections in the theta band.

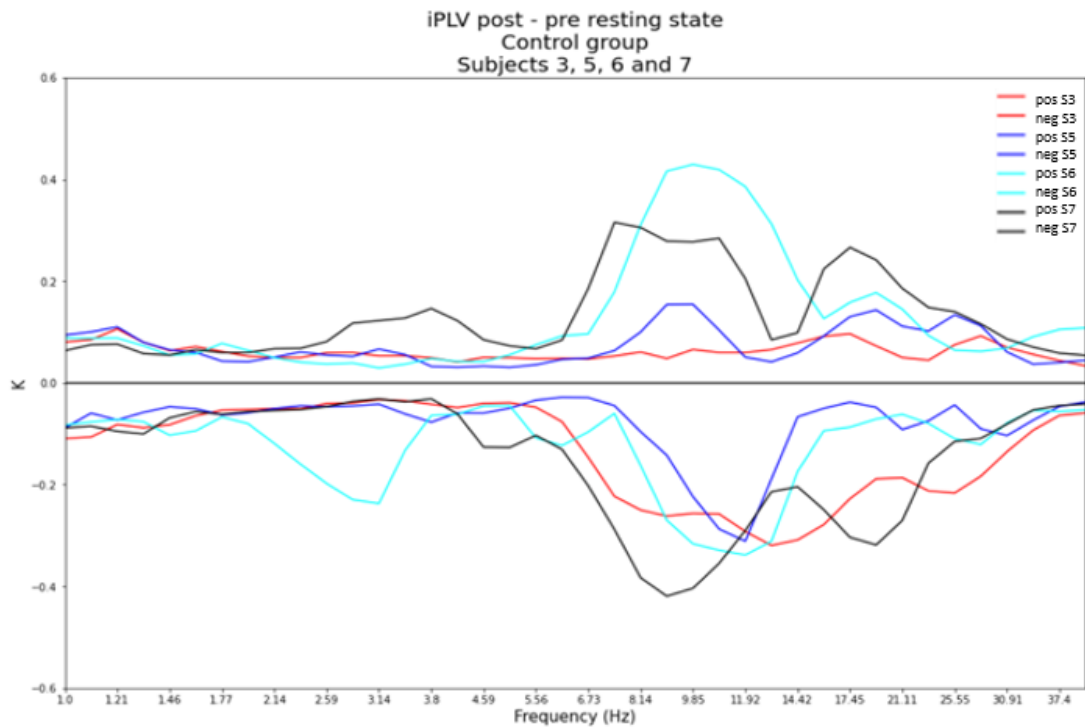


Figure 18. Connection density  $K$  as a function of frequency Hz. Single-subject iPLV values. Post and pre resting state measurement from the control group.

In the control group, subject 6 and 7 showed larger positive connections in the alpha band, whereas subject 5 showed small enhancement in the alpha band. All participants showed small enhancement in the positive connection in the beta band. Subject 3 did not show positive connection peaks in any frequency band. All participants had large negative connection in the alpha band. Noticeable difference between active and control groups in a single subject level, was that active group showed larger density peaks in more variety of frequency bands.

## 5 Discussion

Main aim of this study was to investigate whether active group showed phase-synchronization differences to control group. The extent of synchrony was estimated with connection density  $K$ , which is the proportion of significant interactions from all possible interactions among brain areas (Palva and Palva. 2012; Hirvonen et al. 2017).

Most interestingly, the frequency spectrum of  $K$  showed that synchronization in the alpha ( $\alpha$ , 8 – 12 Hz) band was strengthened whiting the active group. Also, small strengthening delta ( $\delta$ , 1 - 3 Hz) and theta ( $\theta$ , 4 – 8 Hz) synchronization was shown whiting the active group. Interestingly, frequency spectrum of  $K$  showed that synchronization in theta ( $\theta$ , 4 – 8 Hz) band was weakened for active group and alpha ( $\alpha$ , 8 – 12 Hz) band was weakened for the control group. In a single subject level, all participants showed positive connections in alpha ( $\alpha$ , 8 – 12 Hz) frequency band in both groups and some enhancements in the theta ( $\theta$ , 4 – 8 Hz) band within the active group.

It is known from literature that WM performance is shown as a strengthened frequency range from theta (Solomon et al. 2017) to higher beta band (Laukka et al. 1995). In the case of CC, recordings in the frontal cortex show oscillations in the beta band (20–30 Hz) (Buschman et al. 2007). Enhanced beta band activity is linked to control of behavior and representing rules (Stoll et al. 2015). Studies have recognized enhanced theta band activity in the medial-frontal cortex, that is linked in monitoring (Ullsperger et al. 2014), whereas enhanced theta band in medial-cortex and lateral-frontal regions is linked to control recruitment (Cavanagh et al. 2014). In addition, changes in the alpha band activity has been observed during various cognitive control processes (Palva et al. 2011; Klimesch. 2012).

Decreased activation between pre and post resting states can be interpreted as more efficient processing on trained task, whereas more capacity is left for other processes (Buschkuhl et al. 2012). Decreased activations are linked to increased neural efficiency, where less neurons are needed in well performed tasks (Kelly et al. 2006). Increased activation can be interpreted as an expansion of neural structures that are involved in processing of trained task (Buschkuhl et al. 2012). Thus, badly performed task may activate more neural circuits that are irrelevant to the performance (Kelly et al. 2006). Lower alpha activity can originate from retrieving stored information (Klimesch et al. 2007). Alpha synchronizes in respective brain areas while performing a task, but when the stored information is retrieved, alpha desynchronizes (Klimesch et al. 2007).

Based on the literature review above, strengthened delta, theta and alpha activity on the positive connections can be linked to enhanced cognitive control, whereas strengthened theta band activity on the positive connections can be linked to enhanced working memory within the active group. Negative connections of the active group in the theta and alpha activity indicates decreasing value of the iPLV, where it can be assumed that phase synchrony between parcels is reduced or approaching zero-lag. In addition, desynchronization of theta and alpha frequency in the active group can be interpreted as increased neural efficiency. Negative connections of the control group in the alpha activity indicates decreasing value of the iPLV, what can result from the non-existing cognitive strain on the control paradigm.



In a single subject level in the active group, some subjects showed synchronization in the theta frequency and desynchronization in the alpha frequency. This kind of activity has been studied during a memory formation task (Klimech et al. 1997). In addition, participant's previous game experience (Figure 9) can affect on the activity of certain frequency bands in a single subject level. For example, it is believed that personal experience and expertise can correlate with alpha frequency enhancement (Del Percio et al. 2009).

Results were not false discovery rate (FDR) corrected, where multiple comparisons are corrected and the proportion of false-positives for total number of detections are controlled. The lack of FDR diminishes the power of statistical inference and thus can affect to the results.

## 6 Summary

It is known that human brain can make neuroplastic changes with enhanced activity with computerized cognitive training (Morimoto et al. 2014). These enhancements have been shown to improve cognitive control, task switching and working memory (Morimoto et al. 2014). Goal of this master's thesis was to investigate, whether newly constructed cognitive training paradigm would show differences in neuronal synchronization. There were proven differences in phase-synchronization between the action and control group, where active group enhanced activity in the cognitive control and working memory frequency bands.

Results showed phase synchronization differences already after a short-period of cognitive training, especially in the cognitive control and working memory alpha and theta frequency bands. However, larger participant blocks and more training data are needed to validate these results. In addition, sufficient repetitions and long-term training periods are required to achieve neuroplastic changes. In line with previous acknowledgments, this master's thesis gives promising direction for computerized cognitive training, where paradigms can be utilized as a therapeutics for neurological and psychological disorders.

## References

Achtman, R., Green, S. and Bavelier, D. 2008. Video games as a tool to train visual skills. *Restorative Neurology and Neuroscience*, 26(4-5), pp. 435-46.

Arnulfo, G., Wang, S., Myrov, V., Toselli, B., Hirvonen, J., Fato, M., Nobili, L., Cardinale, F., Rubino, A., Zhigalov A., Palva, S. and Palva, J.M. 2020. Long-range phase synchronization of high-frequency oscillations in human cortex. *Nature Communications* 11, pp. 5363. DOI: 10.1038/s41467-020-18975-8

Barnard, C., Duck, I., Lynn, M. and Timlake, W. 1967. The application of electromagnetic theory to electrocardiology. II. Numerical solution of the integral equations. *Biophysical Journal*, 7(5), pp. 463-491. DOI: 10.1016/S0006-3495(67)86599-8

Beniczky, S. and Schomer, D. 2020. Electroencephalography: basic biophysical and technological aspects important for clinical applications. *Epileptic Disorders*, 22(6), pp. 697-715. DOI: 10.1684/epd.2020.1217

Bruña R., Maestú, F., Pereda, E. 2018. Phase locking value revisited: teaching new tricks to an old dog. *Journal of Neural Engineering*, 15(5). DOI: 10.1088/1741-2552/aacfe4

Buschkuhl, M., Jaeggi, S. and Jonides, J. 2012. Neuronal effects following working memory training. *Developmental Cognitive Neuroscience*, 2(1), pp. 167-179. DOI: 10.1016/j.dcn.2011.10.001.

Buschman, T. and Miller, E. 2007. Top-down versus bottom-up control of attention in the prefrontal and posterior parietal cortices. *Science*, 315(5820), pp. 1860–1862. DOI: 10.1126/science.1138071

Cavanagh, J. and Frank M. 2014. Frontal theta as a mechanism for cognitive control. *Trends in Cognitive Sciences* 18 (2014), pp. 414-421. DOI: 10.1016/j.tics.2014.04.012

Cowan. N. 2014. Working memory underpins cognitive development, learning, and education. *Educational Psychology Review*, 26(2), pp: 197-223. DOI: 10.1007/s10648-013-9246-y

Dariusz, M., Budzik, G. and Jóźwik, J. 2019. Single channel source separation with ICA-based time-frequency decomposition. *Sensors*, 20(7). 2019. DOI: 10.3390/s20072019

Del Percio, C., Babiloni, C., Marzano, N., Iacoboni, M., Infarinato, F., Vecchio, F., et al. 2009. "Neural efficiency" of athletes' brain for upright standing: a high-resolution EEG study. *Brain Research Bulletin*, 79, pp. 193–200. DOI: 10.1016/j.brainres-bull.2009.02.001

Eriksson, J., Vogel, E., Lansner, A., Bergström, F. and Nyberg, L. 2015. Neurocognitive architecture of working memory. *Neuron*. 88(1), pp. 33-46. DOI: 10.1016/j.neuron.2015.09.020

Green, S. and Bavelier, D. 2008. Exercising your brain: a review of human brain plasticity and training-induced learning. *Psychology and Aging*, 23(4), pp. 692-701. DOI: 10.1037/a0014345

Green, S. and Bavelier, D. 2015. Action video game training for cognitive enhancement. *Current Opinion in Behavioral Sciences*, 4, pp. 103-108. DOI: 10.1016/j.cobeha.2015.04.012

Grover, V., Tognarelli, J., Crossey, M., Cox, I., Taylor-Robinson, S., McPhail, M. and Vijay P. 2015. Magnetic resonance imaging: principles and techniques: lessons for clinicians. *Journal of Clinical and Experimental Hepatology*, 5(3), pp. 246-255. DOI: 10.1016/j.jceh.2015.08.001.

Hirvonen J, Wibral M, Palva JM, Singer W, Uhlhaas P, Palva S. 2017. Whole-brain source-reconstructed MEG-data reveal reduced long-range synchronization in chronic schizophrenia. *eNeuro*, 4(5). DOI: 10.1523/ENEURO.0338-17.2017

Hamalainen, M. S., & Ilmoniemi, R. J. 1994. Interpreting magnetic fields of the brain: Minimum norm estimates. *Medical & Biological Engineering & Computing*, 32, pp. 35–42. DOI: 10.1007/BF02512476

Jaeggi, S., Karbach, J. and Strobach, T. 2017. Editorial special topic: Enhancing brain and cognition through cognitive training. *Journal of Cognitive Enhancement* 1, pp. 353–357. DOI: 10.1007/s41465-017-0057-9

Jensen, O., Spaak, E. and Zumer J.M. 2019. Human brain oscillations: from physiological mechanisms to analysis and cognition. *Magnetoencephalography*. Springer, Cham. DOI:10.1007/978-3-030-00087-5\_17

Kelly, C., Foxe, J. and Garavan, H. 2006. Patterns of normal human brain plasticity after practice and their implications for neurorehabilitation. *Archives of Physical Medicine and Rehabilitation*, 87, pp. 20-29. DOI: 10.1016/j.apmr.2006.08.333

Klimesch, W. 2012. Alpha-band oscillations, attention, and controlled access to stored information. *Trends in Cognitive Sciences*, 16(12), pp. 606-617. DOI: 10.1016/j.tics.2012.10.007

Klimesch, W., Doppelmayr, M., Schimke, H. and Ripper, B. 1997. Theta synchronization and alpha desynchronization in a memory task. *Psychophysiology*, 34(2), pp. 169-176. DOI: 10.1111/j.1469-8986.1997.tb02128.x

Klimesch, W., Sauseng, P. and Hanslmayr, S. 2007. EEG alpha oscillations: The inhibition–timing hypothesis. *Brain Research Reviews*, 53(1), pp. 63-88. DOI: 10.1016/j.brainresrev.2006.06.003.

Lachaux, J.P., Rodriguez, E., Martinerie, J. and Varela, F. 1999. Measuring phase synchrony in brain signals. *Human Brain Mapping*, 8(4), pp. 194-208. DOI: 10.1002/(SICI)1097-0193(1999)8:4<194::AID-HBM4>3.0.CO;2-C

Laukka, S., Jarvilehto, T., Alexandrov, I. and Lindqvist, J. 1995. Frontalmidline theta related to learning in a simulated driving task. *Biological Psychology*, 40, pp. 313–332. DOI: 10.1016/0301-0511(95)05122-Q

Meijs J., Weier, O., Peters, M. and van Oosterom, A. 1989. On the numerical accuracy of the boundary element method. *IEEE Transactions on Biomedical Engineering*, 36, pp. 1038–1049. DOI: 10.1109/10.40805

Michel, C. and Brunet, D. 2019. EEG source imaging: a practical review of the analysis steps. *Frontiers in Neurology*, 10, 325. DOI: 10.3389/fneur.2019.00325

Miyake, A., Friedman, N., Emerson, M., Witzki, A., Howerter, A. and Wager, T. 2000. The unity and diversity of executive functions and their contributions to complex “frontal lobe” tasks: a latent variable analysis. *Cognitive Psychology*, 41(1), pp. 49-100. DOI: 10.1006/cogp.1999.0734

Morimoto, S., Wexler, B., Liu, J., Hu, W., Seirup, J. and Alexopoulos, G. 2014. Neuroplasticity-based computerized cognitive remediation for treatment-resistant geriatric depression. *Nature Communications* 5, 4579. DOI: 10.1038/ncomms5579

- Nouchi, R., Taki, Y., Takeuchi, H., Hashizume, H., Nozawa, T. and Kambaram, T. 2013. Brain training game boosts executive functions, working memory and processing speed in the young adults: a randomized controlled trial. *Plos One*, 8(2). DOI: 10.1371/journal.pone.0055518
- Oostenveld, R. and Oostendorp, T. 2002. Validating the boundary element method for forward and inverse EEG computations in the presence of a hole in the skull. *Human Brain Mapping*, 17(3), pp. 179-192. DOI:10.1002/hbm.10061
- Palva, S. and Palva, J.M. 2011. Functional roles of alpha-band phase synchronization in local and large-scale cortical networks. *Frontiers in Psychology*, 2, pp. 204. DOI=10.3389/fpsyg.2011.00204
- Palva, S. and Palva, J.M. 2012. Discovering oscillatory interaction networks with M/EEG: challenges and breakthroughs. *Trends in Cognitive Sciences*, 16(4), pp. 219-230. DOI: 10.1016/j.tics.2012.02.004.
- Palva, J.M., Wang, S., Palva, S., Zhigalov, A., Monto, S., Brookes, M., Schoffelen, J. and Jerbi, K. 2018. Ghost interactions in MEG/EEG source space: A note of caution on inter-areal coupling measures. *NeuroImage*, 173, pp. 623-643. DOI: 10.1016/j.neuroimage.2018.02.032.
- Parro, C., Dixon, M. and Christoff, K. 2018. The neural basis of motivational influences on cognitive control. *Human Brain Mapping*, 39(12), pp. 5097-5111. DOI: 10.1002/hbm.24348
- Riddle, J., Scimeca, J., Cellier, D., Dhanani, S. and D'Esposito, M. 2020. Causal evidence for a role of theta and alpha oscillations in the control of working memory. *Current Biology*, 30(9), pp: 1748-1754. DOI: 10.1016/j.cub.2020.02.065
- Rougier, N., Noelle, D., Braver, T., Cohen, J. and O'Reilly, R. 2005. Prefrontal cortex and flexible cognitive control: Rules without symbols. *Proceedings of the National Academy of Sciences*, 102 (20), pp. 7338-7343. DOI: 10.1073/pnas.0502455102
- Sadaghiani, S. and Kleinschmidt, A. 2016. Brain Networks and  $\alpha$ -Oscillations: Structural and Functional Foundations of Cognitive Control. *Trends in Cognitive Sciences*, 20(11), pp. 805-817. DOI: 10.1016/j.tics.2016.09.004
- Sauseng, P. and Liesefeld, H. 2020. Cognitive control: brain oscillations coordinate human working memory. *Current Biology*, 30(9), 405-407. DOI: 10.1016/j.cub.2020.02.067

Schmidt, B., Ghuman, A. and Huppert T. 2014. Whole brain functional connectivity using phase locking measures of resting state magnetoencephalography. *Frontiers in Neuroscience*, 8, 141. DOI: 10.3389/fnins.2014.00141

Siegel, M., Donner, T. and Engel, A. Spectral fingerprints of large-scale neuronal interactions. 2012. *Nature Reviews Neuroscience* 13, pp. 121–134. DOI: 10.1038/nrn3137

Solomon, E., Kragel, J. and Sperling, M.R. 2017. Widespread theta synchrony and high-frequency desynchronization underlies enhanced cognition. *Nature Communications* 8, pp. 1704 (2017). DOI: 10.1038/s41467-017-01763-2

Sousa, D., and Hart, L. 2011. The physiology of the brain. *Educational neuroscience*. pp. 3-28. DOI: 10.4135/9781483387734.n1

Stoll, F., Wilson, C., Faraut, M., Vezoli, J., Knoblauch, K. and Procyk, E. 2016. The effects of cognitive control and time on frontal beta oscillations. *Cerebral Cortex*, 26(4), p. 1715–1732, DOI: 10.1093/cercor/bhv006

Ullsperger, M., Fischer, A., Nigbur, R. and Endrass, T. 2014. Neural mechanisms and temporal dynamics of performance monitoring. *Trends in Cognitive Sciences*, 18(5), p. 259-267. DOI: 10.1016/j.tics.2014.02.009

Varela, F., Lachaux, J. P., Rodriguez, E. and Martinerie, J. 2001. The brainweb: phase synchronization and large-scale integration. *Nature Reviews Neuroscience* 2, pp. 229–239. DOI: 10.1038/35067550

Wang, C., Jaeggi, S., Yang, L., Zhang, T., He, X., Buschkuhl, M. and Zhang, O. 2019. Narrowing the achievement gap in low-achieving children by targeted executive function training. *Journal of Applied Developmental Psychology*, 63, pp. 87-95. DOI: 10.1016/j.appdev.2019.06.002

Wang, S., Lobier, M., Siebenhühner, F., Puoliväli, T., Palva, S. and Palva, J.M. 2018. Hyperedge bundling: A practical solution to spurious interactions in MEG/EEG source connectivity analyses. *NeuroImage*, 173, pp. 610-622, DOI: 10.1016/j.neuroimage.2018.01.056.

Waris, O., Jaeggi, S., Seitz, A., Lehtonen, M., Soveri, A., Lukasik, K., Söderström, U., Hoffing, R. and Laine, M. 2019. Video gaming and working memory: A large-scale cross-sectional correlative study. *Computers in Human Behavior*, 97, pp. 94-103. DOI: 10.1016/j.chb.2019.03.005

Yoshinaga, K., Matsushashi, M., Mima, T., Fukuyama, H., Takahashi, R., Hanakawa, T. and Ikeda, A. 2020. Comparison of phase synchronization measures for identifying stimulus-induced functional connectivity in human magnetoencephalographic and simulated data. *Frontiers in Neuroscience*, 14, 648. DOI: 10.3389/fnins.2020.00648

Zelazo, P. and Carlson, S. 2012. Hot and cool executive function in childhood and adolescence: Development and plasticity. *Child Development Perspectives*, 6(4), pp.354-360. DOI: 10.1111/j.1750-8606.2012.00246.x